

# Fabrication of “Roll-off” and “Sticky” Superhydrophobic Cellulose Surfaces via Plasma Processing

Balamurali Balu, Victor Breedveld,\* and Dennis W. Hess\*

School of Chemical and Biomolecular Engineering, Georgia Institute of Technology, 311 Ferst Drive, Atlanta, Georgia 30332-0100

Received December 1, 2007. In Final Form: January 10, 2008

Most of the artificial superhydrophobic surfaces that have been fabricated to date are not biodegradable, renewable, or mechanically flexible and are often expensive, which limits their potential applications. In contrast, cellulose, a biodegradable, renewable, flexible, inexpensive, biopolymer which is abundantly present in nature, satisfies all the above requirements, but it is not superhydrophobic. Superhydrophobicity on cellulose paper was obtained by domain-selective etching of amorphous portions of the cellulose in an oxygen plasma and subsequently coating the etched surface with a thin fluorocarbon film deposited via plasma-enhanced chemical vapor deposition using pentafluoroethane as a precursor. Variation of plasma treatment yielded two types of superhydrophobicity: “roll-off” (contact angle (CA),  $166.7^\circ \pm 0.9^\circ$ ; CA hysteresis,  $3.4^\circ \pm 0.1^\circ$ ) and “sticky” (CA,  $144.8^\circ \pm 5.7^\circ$ ; CA hysteresis,  $79.1^\circ \pm 15.8^\circ$ ) near superhydrophobicity. The nanometer scale roughness obtained by delineating the internal roughness of each fiber and the micrometer scale roughness which is inherent to a cellulose paper surface are robust when compared to roughened structures created by traditional polymer grafting, nanoparticle deposition, or other artificial means.

## 1. Introduction

It has long been recognized that superhydrophobic surfaces<sup>1</sup> (water contact angle (CA)  $> 150^\circ$ ) require a unique combination of two fundamental properties: (1) surface roughness and (2) low surface energy. So far superhydrophobic surfaces have been fabricated in a variety of lengths, e.g., single lengthscale (nanometer range<sup>2–4</sup> or micrometer range<sup>5–7</sup>) or hierarchical combination of length scales (micrometer–micrometer<sup>8</sup> or micrometer–nanometer<sup>9–11</sup>) with various topographies. Since the late 1930s, significant interest has existed in designing water-repellant surfaces by artificially generating these two properties on a variety of materials. From a processing viewpoint, the desired combination can be obtained via several routes: (1) add roughness to an inherently low-surface-energy material, (2) add roughness to a hydrophilic surface and then modify it with a hydrophobic surface treatment, or (3) modify a surface with a low-surface-energy material which adds inherent roughness, for example, the deposition of hydrophobic nanoparticles. Surface roughness at nano- and micrometer scales has been obtained through a variety of methods: controlled crystallization,<sup>12</sup> plasma etching,<sup>13</sup> laser

etching,<sup>14</sup> plasma-enhanced chemical vapor deposition (PECVD),<sup>15</sup> lithography,<sup>16</sup> electro-spinning and -spraying,<sup>17</sup> sol–gel processing,<sup>18</sup> stretching,<sup>19</sup> nanocasting,<sup>20</sup> and graft-on-graft polymerization.<sup>21</sup> Similarly, there are numerous ways to modify the surface chemistry, such as sol–gel processing,<sup>18</sup> graft polymerization,<sup>21</sup> electrochemical deposition,<sup>22</sup> PECVD,<sup>23</sup> chemical vapor deposition,<sup>13</sup> and atomic layer deposition.<sup>24</sup> The selection of the appropriate method to create roughness and/or low surface energy depends on the mechanical and physiochemical properties of the substrate.

Artificial superhydrophobic surfaces have been fabricated on a variety of organic and inorganic substrates, e.g., polymers,<sup>8,13,25–27</sup> Si wafers,<sup>5,9,11</sup> glass slides,<sup>10,28</sup> and metals.<sup>29,30</sup> With the increased environmental interest in the use of

\* To whom correspondence should be addressed. E-mail: victor.breedveld@chbe.gatech.edu (V.B.); dennis.hess@chbe.gatech.edu (D.W.H.). Phone: +1-404-894-5134 (V.B.); +1-404-894-5922 (D.W.H.). Fax: +1-404-894-2866 (V.B.); +1-404-894-2866 (D.W.H.).

(1) Li, X. M.; Reinhoudt, D.; Crego-Calama, M. *Chem. Soc. Rev.* **2007**, *36*, 1529–1529.

(2) Martines, E.; Seunarine, K.; Morgan, H.; Gadegaard, N.; Wilkinson, C. D. W.; Riehle, M. O. *Nano Lett.* **2005**, *5*, 2097–2103.

(3) Feng, L.; Li, S. H.; Li, H. J.; Zhai, J.; Song, Y. L.; Jiang, L.; Zhu, D. B. *Angew. Chem., Int. Ed.* **2002**, *41*, 1221.

(4) Hosono, E.; Fujihara, S.; Honma, I.; Zhou, H. S. *J. Am. Chem. Soc.* **2005**, *127*, 13458–13459.

(5) Oner, D.; McCarthy, T. J. *Langmuir* **2000**, *16*, 7777–7782.

(6) Gao, L. C.; McCarthy, T. J. *Langmuir* **2006**, *22*, 6234–6237.

(7) Bico, J.; Marzolin, C.; Quere, D. *Europhys. Lett.* **1999**, *47*, 220–226.

(8) Gao, L. C.; McCarthy, T. J. *Langmuir* **2006**, *22*, 5998–6000.

(9) Gao, L. C.; McCarthy, T. J. *Langmuir* **2006**, *22*, 2966–2967.

(10) Xiu, Y. H.; Zhu, L. B.; Hess, D. W.; Wong, C. P. *Langmuir* **2006**, *22*, 9676–9681.

(11) Zhu, L. B.; Xiu, Y. H.; Xu, J. W.; Tamirisa, P. A.; Hess, D. W.; Wong, C. P. *Langmuir* **2005**, *21*, 11208–11212.

(12) Lu, X. Y.; Zhang, C. C.; Han, Y. C. *Macromol. Rapid Commun.* **2004**, *25*, 1606–1610.

(13) Teshima, K.; Sugimura, H.; Inoue, Y.; Takai, O.; Takano, A. *Appl. Surf. Sci.* **2005**, *244*, 619–622.

(14) Jin, M. H.; Feng, X. J.; Xi, J. M.; Zhai, J.; Cho, K. W.; Feng, L.; Jiang, L. *Macromol. Rapid Commun.* **2005**, *26*, 1805–1809.

(15) Chen, W.; Fadeev, A. Y.; Hsieh, M. C.; Oner, D.; Youngblood, J.; McCarthy, T. J. *Langmuir* **1999**, *15*, 3395–3399.

(16) Callies, M.; Chen, Y.; Marty, F.; Pepin, A.; Quere, D. *Microelectron. eng.* **2005**, *78*, 100–105.

(17) Jiang, L.; Zhao, Y.; Zhai, J. *Angew. Chem., Int. Ed.* **2004**, *43*, 4338–4341.

(18) Shirtcliffe, N. J.; McHale, G.; Newton, M. I.; Perry, C. C.; Roach, P. *Chem. Commun.* **2005**, 3135–3137.

(19) Zhang, J. L.; Li, J. A.; Han, Y. C. *Macromol. Rapid Commun.* **2004**, *25*, 1105–1108.

(20) Sun, T. L.; Feng, L.; Gao, X. F.; Jiang, L. *Acc. Chem. Res.* **2005**, *38*, 644–652.

(21) Nystrom, D.; Lindqvist, J.; Ostmark, E.; Hult, A.; Malmstrom, E. *Chem. Commun.* **2006**, 3594–3596.

(22) Zhang, X.; Shi, F.; Yu, X.; Liu, H.; Fu, Y.; Wang, Z. Q.; Jiang, L.; Li, X. Y. *J. Am. Chem. Soc.* **2004**, *126*, 3064–3065.

(23) Sahin, H. T.; Manolache, S.; Young, R. A.; Denes, F. *Cellulose* **2002**, *9*, 171–181.

(24) Sinha, A.; Hess, D. W.; Henderson, C. L. *J. Vac. Sci. Technol., B* **2006**, *24*, 2523–2532.

(25) Teshima, K.; Sugimura, H.; Inoue, Y.; Takai, O.; Takano, A. *Chem. Vap. Deposition* **2004**, *10*, 295–+.

(26) Lee, J. A.; McCarthy, T. J. *Macromolecules* **2007**, *40*, 3965–3969.

(27) Youngblood, J. P.; McCarthy, T. J. *Macromolecules* **1999**, *32*, 6800–6806.

(28) Chang, K. C.; Chen, Y. K.; Chen, H. *J. Appl. Polym. Sci.* **2007**, *105*, 1503–1510.

(29) Qian, B. T.; Shen, Z. Q. *Langmuir* **2005**, *21*, 9007–9009.

(30) Li, M.; Xu, J. H.; Lu, Q. H. *J. Mater. Chem.* **2007**, *17*, 4772–4776.

renewable resources and biodegradable materials, the inorganic substrates listed above are less than ideal. Moreover, they are not mechanically flexible, which limits their processability and therefore the range of potential applications. Organic polymer substrates, on the other hand, are flexible, but they tend to be fairly expensive and often lack biodegradability and renewability. Hence, the search for alternative substrates for superhydrophobic surfaces is ongoing. Cellulose, a biodegradable, renewable, inexpensive, biopolymer, which is abundantly present in nature, has been targeted as a candidate. If cellulose-based paper substrates can be rendered superhydrophobic by simple processing schemes, they will offer a promising alternative to conventional superhydrophobic substrates. Due to relatively low cost and mechanical flexibility, these surface-modified materials could have applications in a vast array of products, including fast food and microwavable food packages, beverage containers, self-cleaning cartons, labels, paper boards, heat-transfer surfaces (to remove condensed water quickly), microfluidic devices, and membranes with low degrees of surface fouling.

Untreated cellulose-based paper is hydrophilic and readily absorbs water. But previous studies suggest that surface treatments can be used to make cellulose fibers hydrophobic.<sup>23,31–34</sup> In those studies, although modification of the cellulose fibers with thin hydrophobic layers increased the CA (hydrophobicity), superhydrophobicity was not achieved due to the absence of appropriate roughness scales. Paper surfaces have micrometer roughness due to the network of overlapping fibers but lack the smaller nanoscale roughness that is usually associated with superhydrophobicity. Unfortunately, cellulose fibers represent a relatively complex substrate and their properties, in particular their water absorbency, stretchability, compressibility, porosity, nonuniform surface chemistry, and thermal degradability, inhibit the use of most of the commonly used techniques for creating smaller characteristic length scales (see above discussion). In one study, in-situ atom transfer radical polymerization (ATRP) has been used<sup>21</sup> to graft and grow a polymer layer with nanoscale roughness on a fiber surface, which led to superhydrophobicity (water CAs > 160°). However, because the nanoscale roughness of grafted substrates is associated with a deformable polymer film, robustness and durability are limited. Therefore, it would be advantageous to change the surface topography of cellulose fibers inherently, instead of achieving roughness via the deposited surface layer. To proceed in this direction, it is essential to understand the internal structure of cellulose fibers; considerable information has been published on this topic.<sup>35–41</sup> It is widely accepted that each cellulose fiber consists of several microfibril bundles, which in turn are composed of microfibrils, with diameters ranging from 3 to 30 nm.<sup>35,36,38,40</sup> In combination with the already mentioned micrometer lengthscale of the fiber

network, the microfibrils could provide the necessary additional lengthscale for superhydrophobicity. Because the surface of native cellulose fibers is relatively smooth, the challenge is to find a method to expose the microfibrils and thus roughen the surface. One key characteristic of the microfibrils is that they contain mostly crystalline cellulose moieties, while the matrix surrounding the microfibrils is predominantly amorphous in nature.<sup>35–37,42</sup> Taking advantage of this inherent difference in material properties may offer a viable approach to generate superhydrophobicity on cellulose surfaces.

Domain-selective etching has been used to create surface roughness in polymer substrates with crystalline and amorphous domains.<sup>13,27,43,44</sup> In these studies, etching was performed by a vapor-phase plasma process at low temperature, under solvent-free conditions. Selectivity is based on the premise that amorphous domains of polymer substrates will be more susceptible to reactive plasma etching than crystalline domains. Etching thus preferentially erodes the amorphous domains, leaving behind the crystalline domains. This process ultimately results in a roughened polymer surface with a characteristic lengthscale that is determined by the size of and distance between crystalline domains. Because of the difference in crystallinity between microfibrils and surrounding matrix, the hypothesis is that selective etching should be possible on cellulose fibers, provided that the appropriate etching conditions are generated. Previous studies applied plasma-assisted etching of paper surfaces to investigate interfiber bonding, internal structures of fibers, and coating distribution within the paper.<sup>45</sup> The focus of their work was to establish plasma processing conditions that were aggressive (using CF<sub>4</sub> and O<sub>2</sub> gases), so that the etching process served as a fine microtome to generate a z-directional cross-section of the paper for analysis of various properties with respect to depth. Our study focused on surface modification (altering only the top layers of fibers) while maintaining bulk paper properties. As a result, our investigation invoked considerably less aggressive plasma etching conditions to achieve selective etching of the surface layers of cellulose fibers in order to generate appropriate roughness scales for superhydrophobicity. However, as discussed in the introduction, roughness is not sufficient to establish superhydrophobicity. The inherently hydrophilic cellulose fibers must also be hydrophobized. To modify the etched fibers, we relied on previous work that employed PECVD of a fluorocarbon coating.<sup>32–34,46</sup>

In this paper we demonstrate that superhydrophobic properties can be created on paper surfaces via a combination of selective etching by an oxygen plasma and deposition of a fluorocarbon film (~100 nm on Si wafer) from pentafluoroethane (PFE) via PECVD. Because both steps alter primarily the surface properties of cellulose fibers, it is expected that the bulk material properties remain unchanged. Also, because the approach relies on uncovering roughness present inherently on cellulose fibers, the roughness obtained by this approach should be more mechanically robust than roughness obtained from grafted polymers that has been used previously to impart superhydrophobicity to paper.

## 2. Experimental Section

**2.1. Materials.** *2.1.1. Substrates.* Three different substrates have been employed. (1) Standard copy-grade paper (Office Depot;

- (31) Cunha, A. G.; Freire, C. S. R.; Silvestre, A. J. D.; Neto, C. P.; Gandini, A.; Orblin, E.; Fardim, P. *Biomacromolecules* **2007**, *8*, 1347–1352.  
 (32) Mukhopadhyay, S. M.; Joshi, P.; Datta, S.; MacDaniel, J. *Appl. Surf. Sci.* **2002**, *201*, 219–226.  
 (33) Mukhopadhyay, S. M.; Joshi, P.; Datta, S.; Zhao, J. G.; France, P. *J. Phys. D: Appl. Phys.* **2002**, *35*, 1927–1933.  
 (34) Vaswani, S.; Koskinen, J.; Hess, D. W. *Surf. Coat. Technol.* **2005**, *195*, 121–129.  
 (35) Ranby, B. *Adv. Chem. Ser.* **1969**, 139.  
 (36) Zhao, H. B.; Kwak, J. H.; Zhang, Z. C.; Brown, H. M.; Arey, B. W.; Holladay, J. E. *Carbohydr. Polym.* **2007**, *68*, 235–241.  
 (37) Deraman, M.; Zakaria, S.; Murshidi, J. A. *Jpn. J. Appl. Phys., Part 1* **2001**, *40*, 3311–3314.  
 (38) Manley, R. S. J. *Nature* **1964**, *204*, 1155–&  
 (39) Simon, I.; Glasser, L.; Scheraga, H. A.; Manley, R. S. *Macromolecules* **1988**, *21*, 990–998.  
 (40) Ranby, B.; Rydholm, S. A. *High Polymers*; Interscience: New York 1956; Vol. 10, p 351.  
 (41) Smook, G. A. *Handbook of Pulp and Paper Technology*; Wangus Wilde Publications: Vancouver, Bellingham, 1990.

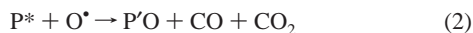
- (42) McKeown, J. J.; Lyness, W. I. *J. Polym. Sci.* **1960**, *47*, 9–17.  
 (43) Kim, S.; Lee, K. J.; Seo, Y. *Langmuir* **2004**, *20*, 157–163.  
 (44) Teshima, K.; Sugimura, H.; Inoue, Y.; Takai, O.; Takano, A. *Langmuir* **2003**, *19*, 10624–10627.  
 (45) Sapieha, S.; Wrobel, A. M.; Wertheimer, M. R. *Plasma Chem. Plasma Processing* **1988**, *8*, 331–346.  
 (46) Denes, F.; Hua, Z. Q.; Barrios, E.; Young, R. A.; Evans, J. J. *Macromol. Sci., Pure Appl. Chem.* **1995**, *A32*, 1405–1443.

“Premium white copy paper”; brightness: 104, weight 76 g/m<sup>2</sup>), (2) handsheets, control paper substrates without filler particles or other additives, and (3) silicon wafers as well-defined model substrates. Handsheets were prepared using TAPPI standardized method T205 sp-02: dry sheets of soft and hard wood fibers (1:1 mass ratio) were soaked overnight, beaten to a pulp in a valley beater, and diluted to appropriate consistency; the pulp is poured into a mesh-bottom mold, and the water is allowed to drain under gravity to form a handsheet, which is then pressed between blotter paper sheets and further dried in a hot press.

**2.1.2. Plasma Reactor Reagents.** PFE monomer gas (N4 grade, 99.99%) was kindly donated by Dr. Mike Mocella from Dupont (Wilmington, DL). Argon carrier gas (Ultra High Purity, 99.99%) was purchased from Air Products and Chemicals Inc. (Allentown, PA). Nitrogen (Ultra High Purity, 99.999%) and oxygen (Ultra Pure Carrier, 99.996%) were purchased from Airgas Inc. (Radnor, PA).

**2.2. Plasma Processing.** A 6 in. parallel plate plasma reactor was used for the plasma processing. The stainless steel bottom electrode was grounded and heated to 110 °C using Omegalux CIR 2015 cartridge heaters (Omega Engineering Inc., Stamford, CT). The temperature at the bottom electrode was monitored using a type K thermocouple controlled by a Syskon RKC temperature controller (RKC Instrument Inc., South Bend, IN). The stainless steel top electrode of the reactor was connected to a HF-300 13.56 MHz, RF power supply (ENI Power Systems, Rochester, NY). To minimize reflected power in the plasma reactor a matching network (Heathkit SA-2060A, Heath Company, Benton Harbor, MI) was placed between the top electrode and the power supply. The reactor pressure was monitored and maintained using a pressure gauge (Varian Inc., Lexington, MA) and an Alcatel 2063 C rotary vacuum pump (Alcatel, Annecy, France). Additional details of this reactor can be found elsewhere.<sup>34</sup> The plasma process for surface modification of the substrates consisted of two steps: (1) reactive etching in an oxygen plasma and (2) fluorocarbon deposition.

**2.2.1. Etching.** After placing a sample on the heated lower electrode, the reactor was evacuated to base pressure (~20 mTorr) and oxygen flow initiated at a flow rate of 6 sccm. After the reactor reached a stable (steady state) pressure (~100 mTorr), an RF power of 150 W was applied to the top electrode for 30 min. At the end of the plasma treatment, the oxygen flow was terminated and the reactor was again evacuated to base pressure. The relatively low pressure and high power combination was somewhat arbitrarily selected with the aim to enhance the cellulose etch rate and promote domain selective etching. Etching proceeds by reaction of oxygen species (primarily O\* and O\*) with cellulose (P) to form water vapor, CO, and CO<sub>2</sub>, thereby removing material from the surface according to the following reactions:<sup>45</sup>



**2.2.2. Deposition.** A thin film of fluorocarbon was then deposited onto the substrates. The deposition gas mixture consisted of a precursor gas (PFE flowing at 20 sccm) and a carrier gas (argon flowing at 75 sccm). After the reactor reached a stable (steady state) pressure (1 Torr), an RF power of 120 W was applied to the top electrode for 2 min. Electron impact collisions with the precursor form various C<sub>x</sub>F<sub>y</sub>H<sub>z</sub> moieties, which react primarily at the substrate surface to form an adherent cross-linked fluorocarbon film.<sup>33,34,47</sup> At the end of the deposition, the plasma power was turned off and the reactor evacuated to base pressure. Finally, the reactor was repressurized to atmospheric pressure by backfilling with N<sub>2</sub> gas and the sample was removed from the reactor for surface characterization. Under these conditions, the thickness of the deposited fluorocarbon film on a silicon wafer, which can readily be measured via ellipsometry, was ~100 nm. The full process, including Steps 1 (etching) and 2 (deposition) will be referred to as

superhydrophobic (SH)-treatment in this report. Control experiments, designated SH-control-treatment, were performed in which the samples were processed similar to SH-treatment, but without striking the plasma in the etching step (1). These experiments were designed to isolate the effect of processing conditions (oxygen exposure, exposure to vacuum, heating) from the actual etching. In addition to these control studies, some samples were only exposed to Step 2 (fluorocarbon deposition), eliminating Step 1 entirely; this third treatment is termed PFE-treatment.

**2.3. Characterization.** **2.3.1. SEM.** SEM measurements were obtained with a LEO scanning electron microscope (model 1530) operated at a pressure of ~1.0 × 10<sup>-7</sup> Torr at room temperature. The operation voltage was adjusted between 5 and 10 kV depending on the magnifications used to avoid damaging the paper samples. Since both the paper and PFE film are insulators, the substrates were sputter coated (EMS 350) with a thin film of gold (~20 nm) prior to SEM measurements.

**2.3.2. X-ray Photoelectron Spectroscopy (XPS).** Spectra were collected using a PHI model 1600 spectrometer with Al Kα X-rays. Further details of the this equipment can be found elsewhere.<sup>47</sup>

**2.3.3. Water CA.** Water CA measurements were obtained with a Rame-Hart CA goniometer (model 100). For the static CA measurements, 4 μL water drops were used and still images were recorded and analyzed. Since the adhesion force of the water drops to the PFE-treated paper substrates was very strong, the commonly accepted method for CA hysteresis measurements could not be performed. Because of the strong interactions between the “sticky” near superhydrophobic PFE-treated paper substrates and the water drop, the receding angle decreased with the drop volume in the standard volume-change hysteresis tests. Hence, we adopted a different method: after the static CA measurement, the substrate was slowly moved perpendicular to the needle and the difference between the CA at the advancing and receding contact lines was taken as the CA hysteresis. This method of measuring CA hysteresis was found to be reproducible for the sticky substrates. Moreover, for the SH-treated paper substrate, this method was in agreement with the commonly accepted volume-change method.

### 3. Results and Discussion

**3.1. “Roll-off” and “Sticky” Superhydrophobicity.** Before presenting results, it is appropriate to briefly discuss the definition of superhydrophobicity as used in previous studies. The most common definition for superhydrophobicity is the existence of a static water CA larger than 150°.<sup>48,49</sup> Although the CA is a good descriptor of the interaction between water and solid surfaces, the threshold of 150° is not sufficient to guarantee the water-repellant behavior associated with lotus leaves, i.e., droplet roll-off and self-cleaning. In order to predict the mobility of water droplets, it is also necessary to determine the CA hysteresis, i.e., the difference between advancing and receding CAs at the leading and trailing edge of a moving droplet. It has been found that for a CA hysteresis less than 10°, water drops roll off the surfaces, while for a hysteresis greater than 10° drops tend to stick to the surface, even if such a surface has a CA greater than 150°. In previous publications, surfaces have been considered as superhydrophobic purely on the basis of the criterion of CAs > 150°, with hysteresis values greater than 10°,<sup>5,9,16,50–52</sup> less than 10°,<sup>8,10,11,15,16,26</sup> or even unreported.<sup>13,19,44</sup> A debate exists on whether or not to include the CA hysteresis in the superhydrophobicity definition.<sup>15</sup> In our analysis, we will include both

(48) Ma, M. L.; Hill, R. M. *Curr. Opin. Colloid Interface Sci.* **2006**, *11*, 193–202.

(49) Nakajima, A.; Hashimoto, K.; Watanabe, T. *Monatsh. Chem.* **2001**, *132*, 31–41.

(50) Jin, M. H.; Feng, X. J.; Feng, L.; Sun, T. L.; Zhai, J.; Li, T. J.; Jiang, L. *Adv. Mater.* **2005**, *17*, 1977–+.

(51) Morra, M.; Occhiello, E.; Garbassi, F. *Langmuir* **1989**, *5*, 872–876.

(52) Tadanaga, K.; Katata, N.; Minami, T. *J. Am. Ceram. Soc.* **1997**, *80*, 1040–1042.

(47) Agraharam, S.; Hess, D. W.; Kohl, P. A.; Allen, S. A. *B. J. Vac. Sci. Technol., A* **1999**, *17*, 3265–3271.



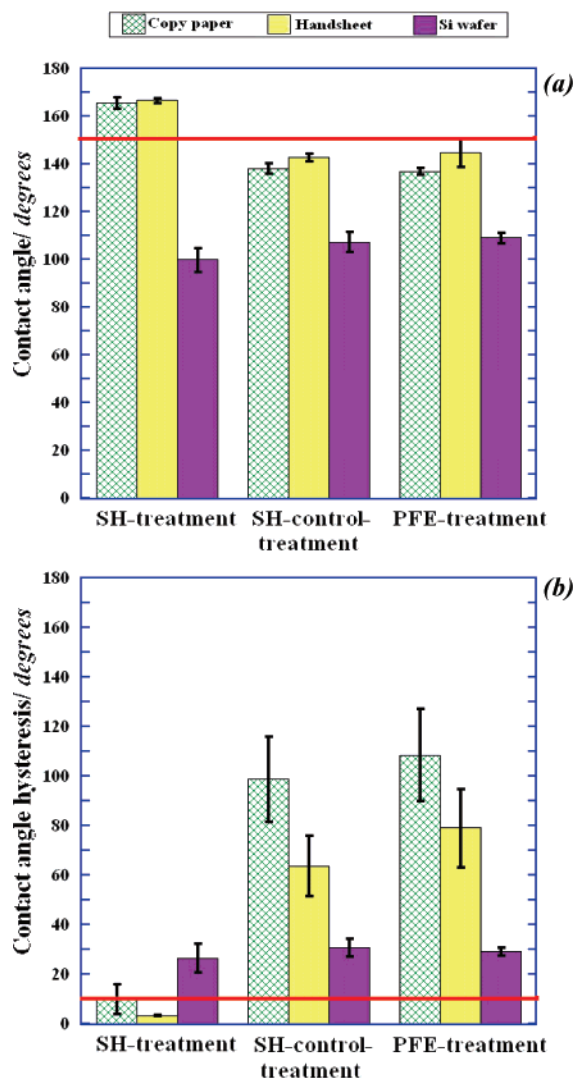


**Figure 1.** Plot of CA (a) and CA hysteresis (b) measurements for the copy paper, handsheets, and Si wafers for the three plasma treatments. Red lines in (a) and (b) indicate the cutoff value for “roll-off” superhydrophobicity. Error bars represent 95% confidence intervals.

the water CA and CA hysteresis to categorize the interactions of hydrophobic substrates with liquids.

The charts in Figure 1 show a comparison of the water CA and CA hysteresis of copy paper, handsheet, and silicon wafer subjected to three tests: (1) SH-treatment, (2) SH-control-treatment, and (3) PFE-treatment. The results for substrates without PFE deposition are not presented in the chart. CA measurements on untreated and oxygen plasma treated (only Step 1 of SH-treatment) copy paper showed a CA of  $81.9^\circ \pm 3.6^\circ$ , while for untreated and oxygen plasma treated handsheets the water drop was absorbed into the paper in less than 1 s, so that the CA could not be measured. Even with the copy paper, slow water absorption takes place, and as a result, CA hysteresis could not be measured for either substrate without PFE deposition. In spite of these challenges, CA measurements clearly revealed the hydrophilic nature of these samples in the absence of fluorocarbon.

The SH-treatment resulted in a water CA  $> 150^\circ$  and CA hysteresis  $< 10^\circ$  for both copy paper and handsheet. These substrates were superhydrophobic according to the classical definition. In comparison, the handsheet and copy paper exposed to PFE-treatment (and SH control treatment) resulted in high CA

**Table 1.** Images of CA and CA Hysteresis Measurements on Handsheets for SH-treatment and PFE-treatment

Treatment	Contact angle	Contact angle hysteresis	Result
SH-treatment			“Roll-off” Superhydrophobic
	$166.7 \pm 0.9$	$3.4 \pm 0.1$	
PFE-treatment			“Sticky” Near Superhydrophobic
	$144.8 \pm 5.7$	$79.1 \pm 15.8$	

( $> 140^\circ$ ) along with large CA hysteresis ( $60\text{--}110^\circ$ ). The fact that both control experiments (SH-control and PFE-treatment) yield the same result for all three substrates proves that the processing conditions (pressure, temperature, and oxygen flow without plasma) of the plasma etching (Step 1) are not the main cause of the observations. To illustrate the difference between the results of SH-treatment and the control experiments, images from the CA and hysteresis measurements on treated handsheet samples are shown in Table 1. Whereas typical “roll-off superhydrophobicity” is observed after SH-treatment with a very low CA hysteresis  $\sim 3.4^\circ$ , the properties of the control sample can best be described as “sticky superhydrophobicity”: the water drop sticks to the surface in spite of exhibiting a very high CA ( $> 140^\circ$ ) with a CA hysteresis  $\sim 79^\circ$ . Although the CA on the control substrates does not strictly meet the stated operational definition of superhydrophobicity ( $> 150^\circ$ ), the 95% confidence interval in our data is within the  $150^\circ$  criteria. Nevertheless, we will characterize this behavior as “sticky near superhydrophobicity”. In the remainder of this paper, we will use the terms roll-off superhydrophobicity (CA  $> 150^\circ$ , hysteresis  $< 10^\circ$ ) and sticky superhydrophobicity (CA  $> 150^\circ$ , hysteresis  $> 10^\circ$ ) to categorize our substrates.

**3.2. Oxygen Plasma Etching of Amorphous Cellulose Domains.** The data in Figure 1 and Table 1 strongly suggest that the SH-treatment generates the desired roughness topography for “roll-off” superhydrophobicity due to etching in the oxygen plasma, but the macroscopic CA measurements do not provide undisputable proof for our hypothesis. To verify the effect of plasma etching (Step 1) and deposition (Step 2) in more detail, high-resolution SEM images were obtained for three samples: (1) untreated handsheets, (2) oxygen etched handsheets (Step 1 of the SH-treatment), and (3) oxygen etched and PFE deposited handsheets (SH-treatment). Figure 2 shows the direct comparison at two SEM magnifications:  $\sim 5000\times$  and  $20\,000\times$ , respectively. It should be noted that the images display single fibers. The fluffy, “cottonlike” surface of the untreated sample can be attributed to the soft amorphous primary layer of the fibers. After oxygen etching, the fibers display a roughened surface with nanometer-scale features (Figure 2c,d) that are not observed on the untreated sample. We attribute the features on the roughened surface to the crystalline portions of the fiber, which remain after selective etching of the amorphous portions of the fibers by the oxygen plasma treatment. XPS studies were performed on the untreated and oxygen etched samples. The O/C ratio of untreated and oxygen etched handsheets were 0.84 and 1.27, respectively, which is consistent with the discussion in Section 2.2. XPS survey scans (data not shown) on the oxygen etched surface displayed only peaks for O1s and C1s, which is expected for cellulose fibers. Moreover, the feature sizes of the

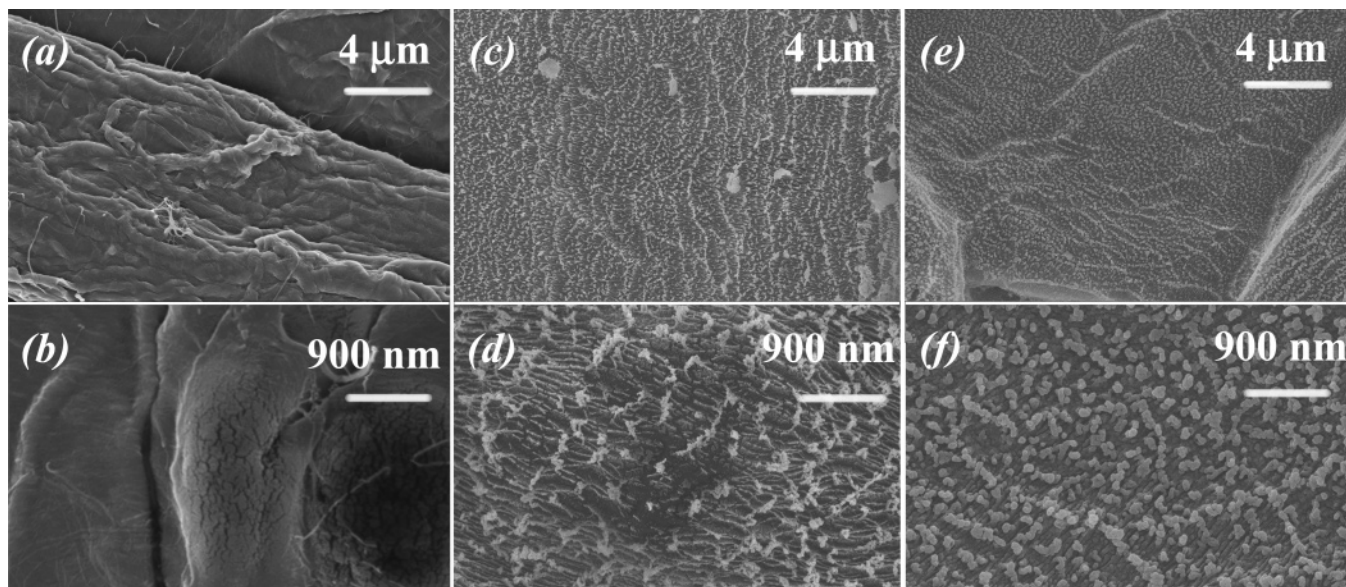


**Figure 2.** High-magnification ( $\sim 5000\times$  and  $\sim 20\,000\times$ ) SEM images of (a,b) “untreated” handsheet fiber, (c,d) oxygen-etched handsheet fiber (Step 1 of SH-treatment), and (e,f) oxygen-etched and PFE-coated handsheet fiber (SH-treatment).

etched sample shown in Figure 2c,d are consistent with the dimensions of crystalline microfibrils,<sup>35–38</sup> which supports our hypothesis. PFE deposition ( $\sim 100$  nm) on the etched surface (Figure 2e,f) accentuates the features present and partially covers ridges created by oxygen etching. Preliminary AFM investigations confirmed the surface topography observed in the SEM pictures. We conclude that the surface roughness created by the SH-treatment is sufficient to generate “roll-off” superhydrophobicity.

**3.3. Significance of the Natural Topography of the Cellulose Fibers for the Two Extreme Behaviors.** The fundamental difference between the SH-treated and control samples (SH-control and PFE-treatment) is that the latter have not been subjected to oxygen etching, which creates nanometer-scale roughness along with the natural micrometer-scale roughness present in the paper surfaces. Since paper is a porous substrate, both samples are considered to be physically heterogeneous (air pockets at the interface) irrespective of their different roughness scales. Thus, the superhydrophobic behavior observed in the “roll-off” and near “sticky” superhydrophobic paper surfaces is expected to be modeled by Cassie’s model,<sup>53</sup> which assumes that a liquid does not completely wet the rough hydrophobic surface and attributes the increased CA to the presence of air pockets (composite surface) at the liquid–solid interface:

$$\cos \theta = f \cos \theta_y - (1 - f) \quad (3)$$

where  $f$  is the wetted area fraction and  $\theta$  and  $\theta_y$  are the apparent and Young’s actual CAs of the surface, respectively. However, recent studies<sup>54</sup> have reported different CAs for the same wetted surface fraction merely by changing surface topography. The variation in CAs was attributed to differences in the contact line topology and tension. Thus, both the three-phase contact line topology and the wetted surface fraction are involved in establishing the CA; such considerations were not addressed by Cassie.<sup>54,55</sup> We therefore conclude that the higher CAs obtained for the “roll-off” and “sticky” superhydrophobic samples are

likely due to the decreased wetted surface fraction and the difference in surface topography which changes the contact line topology.

It has been reported that the hysteresis of a superhydrophobic surface depends upon two properties:<sup>8,56</sup> (1) metastable state energy and (2) barrier energy for the drop to move from one metastable state to another metastable state. These two energies depend on the chemical heterogeneity, contact line topology, roughness, and the wetted fraction of the surface.<sup>6,27</sup> We postulate that the “roll-off” superhydrophobic paper possesses a high metastable state energy and a low barrier energy which may be due to the increased contact line tension and roughness and decreased wetted surface fraction. This energy combination causes water drops to “hop” or “skid” on the surface in search of a lower energy state, thereby causing roll-off with a CA hysteresis of  $3.4^\circ$ . In comparison, we postulate that the “sticky” superhydrophobic paper possesses a relatively low metastable state and a very high barrier energy combination. This may be due to the decreased contact line tension and roughness and increased wetted surface fraction and chemical heterogeneity. As a result, the water drop remains pinned at the initial lower energy location without the ability to move, thereby displaying a CA hysteresis of  $79.1^\circ$ .

Silicon wafers are flat and should not be affected significantly by treatment with oxygen plasma. Indeed, the CA and hysteresis are the same for all three treatments, with higher CA and lower hysteresis than for an untreated sample, as a result of the fluorocarbon coating. It can therefore be concluded that the natural micrometer topography of the paper surface is responsible for the “sticky” superhydrophobicity. In order to obtain “roll-off” superhydrophobicity, a secondary nanoscale roughness must be added, which was achieved by uncovering the implicit nanostructure of microfibrils via oxygen etching. Thus, the natural implicit and explicit roughness present in cellulose fibers plays a critical role in determining whether the paper is “roll-off” or “sticky” superhydrophobic. Both “roll-off” and “sticky” substrates are of considerable interest for applications in which it is important to manipulate the mobility of water droplets; a key question that

(53) Cassie, A. B. D.; Baxter, S. *Trans. Faraday Soc.* **1944**, *40*, 0546–0550.  
 (54) Anantharaju, N.; Panchagnula, M. V.; Vedantam, S.; Neti, S.; Tatic-Lucic, S. *Langmuir* **2007**, *23*, 11673–11676.

(55) Gao, L. C.; McCarthy, T. J. *Langmuir* **2007**, *23*, 3762–3765.

(56) Youngblood, J. P.; McCarthy, T. J. *Abstracts Papers Am. Chem. Soc.* **1999**, *218*, U408–U408.

will be addressed in a future publication is whether it is possible to tune CA hysteresis between these extremes.

**3.4. Robustness and Stability of the Superhydrophobic Paper Substrates.** As discussed previously, a critical property of superhydrophobic paper substrates for practical applications is the robustness of the small micrometer and submicrometer scale features. Even if a substrate is superhydrophobic immediately after creation, several operational factors can affect stability by decreasing the water CA and/or increasing CA hysteresis: condensation of water vapor in the air pockets present at the liquid–solid interface, external pressure applied to the liquid, which compresses the air pockets, and damage to the fragile nanometer-scale features. The first two issues are related to the application in which the substrates will be used. On the other hand, it is expected that the robustness of the roughness generated by our process, which originates from the internal morphology of cellulosic fibers, should be improved relative to that of structures created by traditional polymer grafting or nanoparticle deposition. To confirm this hypothesis, the robustness of the surface was tested with a standardized scotch tape test (ASTM).<sup>57,58</sup> The result was damage to the paper substrate, with a layer of fibers adhering to the scotch tape. Apparently, adhesion failure occurred at fiber–fiber interfaces rather than fiber–PFE interfaces, which demonstrates that the PFE film has excellent adhesive bonding to the fibers. This observation is consistent with the fact that cellulose has numerous –OH moieties which serve as reaction sites for covalent bonding to a cross-linked PFE film. This covalent bonding is stronger than the fiber–fiber hydrogen bonding. After failure of the scotch tape test to confirm the robustness of the topology of the modified surface, we performed another simple wear test on the roll-off superhydrophobic handsheet by pressing it firmly with a bare finger. Although this is not a standardized test, the procedure closely replicates common handling of paper and paperboard and therefore offers insight into practical use of the modified paper surfaces. After this test, the handsheet showed an average CA and CA hysteresis of  $157.1^\circ \pm 4.2^\circ$  and  $21.4^\circ \pm 14.5^\circ$ , respectively, which indicates that the superhydrophobicity was retained. The slight decrease of CA, increase of CA hysteresis, and increased variability of both parameters after the wearability test are likely due to contamination of the surface by grease/dust from the finger, although partial destruction of the nanometer-scale structures cannot be excluded. In addition, CA and CA hysteresis values of SH-treated handsheets and copy paper were constant after storage for several days under ambient conditions ( $T = \sim 25^\circ\text{C}$ , relative humidity =  $\sim 40\%$ ). These studies establish the stability of the PFE film under ambient conditions and thus the inhibition of surface oxidation by atmospheric oxygen.

(57) ASTM Ann. Book ASTM Standards.

(58) Chwa, S. O.; Kim, K. H. *J. Mater. Sci. Lett.* **1998**, *17*, 1835–1838.

## 4. Conclusions

Roll-off superhydrophobic and sticky superhydrophobic surfaces have been prepared on standard hydrophilic paper substrates using plasma processing techniques. The superhydrophobic paper surfaces are robust, flexible, breathable, biodegradable<sup>21</sup> and may also be recyclable. Such conclusions result in part from previous studies in our group that have demonstrated that plasma deposited fluorocarbon films are flexible and breathable.<sup>59</sup> Preliminary studies also suggest that due to the hydrophobic nature of the fluorocarbon layer, the coated fibers can be easily separated in the froth floatation process during paper recycling. Food and Drug Administration (FDA) regulations suggest that fluorine can be used in a water or oil repellent material with a basis weight of 0.22–2.44 g/m<sup>2</sup> depending upon the chemical form in which it is present.<sup>60</sup> On the basis of these regulations, we conclude that the 100 nm film on a paper substrate with a basis weight of  $\sim 76$  g/m<sup>2</sup> (typical for a copy paper) will fall within the limits specified even if the fluorine is not fully removed when the paper is recycled. To our knowledge, the combination of the above-discussed properties (robustness, flexibility, breathability, biodegradability, renewability, and recyclability) has not been reported to date for superhydrophobic surfaces, and in particular, not for a commodity product like paper. Hence, we expect that the approach described to fabricate superhydrophobic paper surfaces may lead to applications of superhydrophobic substrates that were thus far uneconomical. Specifically, these results should find application in packaging, printing, de-inking (paper recycling), biomedical, and chemical industries.

**Acknowledgment.** The authors thank Dr. Mike Mocella (Dupont) for generously donating the PFE gas, Umamaheshwari Udayasankar (Institute for Paper Science and Technology (IPST) at Georgia Tech) for performing SEM studies, Yonghao Xiu (Georgia Tech) for support with SEM and CA measurements, and Dr. Timothy Patterson (IPST/Georgia Tech) for useful discussions. B.B. thanks IPST for fellowship support.

**Note Added after ASAP Publication.** This article was published ASAP on March 4, 2008. A change has been made to equation 3. The correct version was published on April 29, 2008.

LA703766C

(59) Vaswani, S.; Koskinen, J.; Hess, D. W. *J. Vac. Sci. Technol., A* **2006**, *24*, 1737–1745.

(60) FDA Code of Federal Regulations: Food and Drugs - Indirect Food Additives (Paper and Paper Board Components) **2006**, Title 21 Part 176, 195–234.